Paper No. 959. (quote when citing this article)
Eleventh World Conference on Earthquake Engineering
ISBN: 0 08 042822 3

THE MECHANICS OF ELASTOMERIC SEISMIC ISOLATION BEARINGS

L. J. BILLINGS and R. SHEPHERD

Fluor Daniel, Inc.
3333 Michelson Dr.
Irvine, CA 92730

Earthquake Damage Analysis Corporation
3305 South Woodland Place
Santa Ana, CA 92707

ABSTRACT

Base isolation is a design strategy used to protect facilities from seismic shaking. Adequate methods of predicting, at the design stage, the properties of layered elastomeric isolation bearings under compression and shear loads are still under development. No methods were available for predicting the stresses in the internal steel shims of bearings configured with central holes prior to the work presented in his paper.

Sophisticated, nonlinear, finite element analysis (FEA) techniques are described by which individual isolators are modeled. Direct shear tests were conducted on samples of the rubber, and various constitutive elastomeric models are investigated. A three parameter model introduced by Yeoh was implemented into the finite element analyses. The models included nonlinear material, geometry and boundary effects.

Direct compression and direct compression plus shear were applied to the finite element models. The internal stresses determined in the steel shims under both compression and compression plus shear are presented. Various geometry configurations were investigated including various central hole diameters. When comparing bearings with central holes, a solid configuration and a bearing with a central hole filled with rubber were included along with four different hole diameters.

As a result of this investigation, the mechanics of the behavior of multilayered elastomer and steel isolation bearings subjected to large shear strains are better understood. An improved design curve for bearings with central holes is provided. Currently available, simplified, closed form equations for predicting bearing mechanics are validated.

KEYWORDS

Elastomeric; bearing; large strain; finite element; nonlinear; Mooney; Yeoh; base isolation;

BACKGROUND

Some accepted design equations are subjected to a critical comparison with the FEA predictions. The strengths and shortcomings of the equations may then be exposed. FEA is particularly useful for problems involving complicated geometry and is used to investigate the effects resulting from the presence of a central hole, both empty or plugged with rubber (Billings, 1992). Circular bearings will be considered here, since this geometry not only leads to simpler formulae but is also customary for seismic isolation bearings.

Shear stiffness

The shear stiffness, K_S, of an elastomeric bearing of n layers is given by

$$K_s = \frac{GA}{nh} \tag{1}$$

where G is the shear modulus of the rubber and A is the pad area, πr_S^2 where r_S is the bearing radius. The effect of vertical load on K_S is neglected (Muhr, 1993). Similarly, for a rubber which is linear in stress-strain behavior, K_S is considered to be independent of the shear deflection.

Compression stiffness

The compressive stiffness of a single rubber layer may be expressed as (Gent and Meinecke, 1970),

$$k_c \approx \frac{6GS^2A}{h} \tag{2}$$

where S is a dimensionless quantity often called the "shape factor".

$$S = \frac{r_s}{2h} \tag{3}$$

Small strain elastic theory has been used to calculate the compression stiffness. Since the bulk modulus, K, of rubber is about 2000 MPa, much greater than the shear modulus, G, (typically in the range 0.3 to 3.0 MPa) the original derivations assumed incompressibility (Gent and Meinecke, 1970). Chalhoub and Kelly, (1986), have included the effect of a finite value of K. Equation (2) may be expanded as

$$k_c \approx \frac{A}{h}\left(\frac{1}{6GS^2} + \frac{4}{3K}\right)^{-1} \tag{4}$$

Effect of a Central Hole

Many bearing manufacturers use a steel pin through the central axis of the bearing during the molding and vulcanization process. The pin restrains the reinforcing plates from moving laterally, and conducts heat to the core of the bearing. After molding, the central hole is usually filled with rubber but may just be sealed at each end with a rubber plug (Muhr, 1993). In the case of a central hole of radius r_h in a bearing of radius r_S, Constantinou, et al., (1992) give an equation for compression stiffness:

$$k_c = \frac{6GS^2A}{h} F \tag{5}$$

where

$$A = \pi(r_s^2 - r_h^2) \tag{7}$$

$$S_h = \frac{r_s - r_h}{2h} \tag{6}$$

and F is a slowly increasing function of r_S/r_h, rising from the limiting value of 2/3 at $r_S/r_h = 1$ to 0.80 at $r_S/r_h = 100$ as shown in Fig. 2.

$$F = \left(\frac{r_s}{r_s - r_h}\right)^2 \left\{1 + \left(\frac{r_h}{r_s}\right)^2 + \frac{1 - \left(r_h/r_s\right)^2}{\ln\left(r_h/r_s\right)}\right\} \tag{8}$$

Compression Stiffness

Neglecting compliance of the reinforcing plates and any effect of shear, the compression stiffness of a bearing can be derived from equation (2) by considering n pads to be deformed in series (Thomas, 1983)

$$K_c = \frac{1}{n} k_c \tag{9}$$

FINITE ELEMENT MODELING

The equations given in the previous section are strictly applicable only to small strains. Analytical solutions using large strain theory would give much more complicated expressions. One solution to improving the understanding of the behavior of rubber-steel layered isolators utilizes finite elements. Since elastomeric bearings experience large deformations and the elastomer behaves nonlinearly, the finite element formulation must include geometric and material nonlinearities. In some applications, the elastomer may deform far enough to contact the base plates and the code must allow for such nonlinear boundary conditions.

MARC Analysis Research Corporation's general purpose, nonlinear, finite element code which is designed specifically for nonlinear applications and includes provision for three-dimensional contact and for modeling materials such as elastomers was used in the investigation reported.

Strain-Energy Function

The rubber is represented in the code using a strain energy function $W(I_1, I_2, I_3)$ where I_1, I_2, and I_3 are the strain invariants. If the rubber is assumed incompressible, then W is a function only of I_1 and I_2. For many filled rubbers, $\partial W/\partial I_2$ is much smaller than $\partial W/\partial I_1$, and may be neglected (Yeoh, 1990). The function then becomes, to third order:

$$W = C_{10}(I_1 - 3) + C_{20}(I_1 - 3)^2 + C_{30}(I_1 - 3)^3 \quad (10)$$

where the constants C_{10}, C_{20}, and C_{30} are coefficients requiring specification in the MARC code.

The MARC code assumes near-incompressibility of the rubber, and makes use of the following expression for calculation of the bulk modulus, K (Konter, 1993). K is set by default to,

$$K = (C_{10} + C_{01}) \times 10^4 \quad (11)$$

where C_{01} is the coefficient of $(I_2 - 3)$, set to zero in equation 10.

Simple Shear Test

The stress-strain relation in simple shear was given by Rivlin, (1948) as,

$$\frac{\tau}{\gamma} = 2\left(\frac{\partial W}{\partial I_1} + \frac{\partial W}{\partial I_2}\right) \quad (12)$$

where τ is the shear stress and γ is the shear strain which is related to the invariant I_1 by $\gamma^2 = (I_1 - 3)$. From equations (12) and (10), the stress-strain relation in simple shear may be derived in the form of a quadratic equation in $(I_1 - 3)$ (Treloar, 1975),

$$\frac{\tau}{\gamma} = 2C_{10} + 4C_{20}(I_1 - 3) + 6C_{30}(I_1 - 3)^2 \quad (13)$$

Simple shear test data (Ahmadi, 1991) for the soft, high damping elastomer compound used in the bearings analyzed was plotted as $G = \tau/\gamma$ against $(I_1 - 3) = \gamma^2$. From this curve, a second order equation was fitted using regression analysis. The first few points of the curve had to be neglected to fit the curve with reasonable accuracy. Therefore, the behavior of the elastomer at low strains, especially the high initial stiffness observed in the test corresponding to relatively large G values, is not represented accurately by this model. However, the stiffening effect at large strains is satisfactorily represented. The regression analysis yielded the following constants:

$C_{10} = 0.2031$ Mpa $\quad C_{20} = -0.0132$ Mpa $\quad C_{30} = 0.0018$ MPa

Bearings

The bearings chosen in this analysis were of a type manufactured by Malaysian Rubber Producers' Research Association (MRPRA) for use in research at the Earthquake Engineering Research Center, University of California at Berkeley (Aiken, et al., 1992). The bearings analyzed using the finite element technique had top and bottom metal plates 140 mm in diameter with 4.5 mm thick side cover rubber. There were 12 layers of elastomer of 3.9 mm thick each between the steel shims of 1.56 mm thickness. The steel end plates were 20.2 mm thick and 140 mm diameter. The cover rubber continued up the sides of the end plates. The total height was 104.36 mm. The overall diameter including cover rubber of the basic bearing design was 149 mm and the shape factor was 8.97. FEA was also carried out for bearings modeled on the same design, but with the variations given in Table 1.

Table 1. FEA investigations.

Model	Compression (MPa)
Solid	3.2 to 25.5
6 m hole	5.1
12 mm hole	5.1
12 mm hole filled with elastomer	5.1
24 mm hole	5.1
48 mm hole	5.1

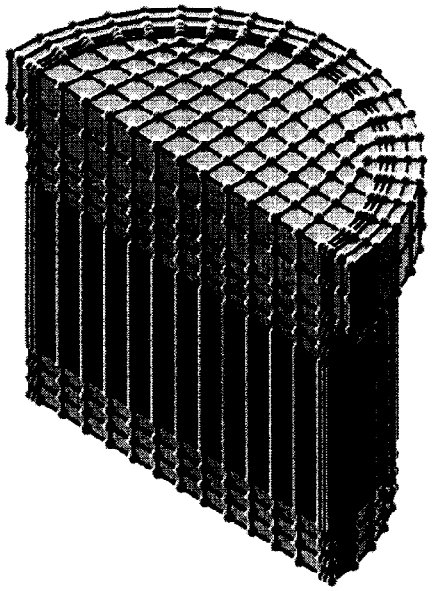

Fig. 1. Solid bearing finite element geometry.

The bearings were first compressed then sheared under their respective compressive pressure until convergence could no longer be achieved. A pressure load was applied over the shim area, followed by point loads on the nodes over the shim area causing shear in the y-direction. The base plate was fixed and x-direction displacement constraints were placed on the plane of symmetry defined by $x = 0$. A typical model consisted of 7472 elements and 8844 nodes for both thick and thin shimmed bearings as shown in Fig. 1.

The cover rubber contacted but did not bond to the connections on either end of the bearing. To model this, the 3D CONTACT option in MARC was used where the bearing was treated as a deformable body fixed to a rigid surface simulating the foundation at its base. To simulate the building frame above the isolator, a thick, stiff, beam was added to the top of the bearing. The nodes on the beam's top surface were all tied to the beam's top center node in the vertical direction with the TYING option to simulate a bolted connection. Consequently, the top of the beam was free to translate in the y and z directions, but constrained from rotating. A crack was left between the top end of the cover rubber and the bottom of the stiff beam. The 3D CONTACT algorithm detected deformable body to deformable body contact in this region.

Each rubber layer had four elements through its thickness and each steel shim had one element through its thickness. The cover rubber had three elements in plan through its thickness. The "assumed strain formulation" option in MARC was invoked for the elements representing the steel shims; the assumption made is that the strain field conformed to that of simple beam theory. This improved the shim bending behavior and allowed use of only one element through the shim thickness to model bending. The steel shims were modeled using a bilinear model with elastic modulus, E = 210,000 MPa, Poisson's ratio, $\nu = 0.29$, and yield stress, $\sigma_y = 325$ MPa. The strain hardening slope was 10,500 MPa. A full Newton-Raphson solution technique was invoked with residual load correction and convergence tolerance on the residuals set to 0.10.

The compressive load was typically applied in 24.5 kN increments. The problem converged readily in compression. Attaining convergence under shear loading was more difficult. The CONTACT option, which modeled the cover rubber to top beam and to foundation surfaces, complicated convergence. The best technique found was to apply steps of approximately 100 N total shear load across the top plate for as many increments as convergence allowed. The computer analysis usually stopped when rubber nodes separated from the rigid or deformable surface. The job was restarted with an automatic stepping procedure to get

Table 2. Stiffnesses of bearings. $G = 0.4061$ MPa and $K = 2030.5$ MPa.

Secant Stiffnesses (kN/mm) under 5.1 MPa Compression				
	K_c FEA	K_c calculated	K_s FEA	K_s calculated
Solid	63.96	64.8	0.101	0.128
6 mm Hole	59.33	46.0	0.102	0.128
12 mm Hole	48.86	40.6	0.100	0.128
12 mm Filled Hole	63.84	64.8	0.102	0.128
24 mm Hole	35.77	32.1	0.093	0.125
48 mm Hole	20.73	18.5	0.066	0.115

through the nodal separation detected by the CONTACT algorithm. Typically, 45 increments were successfully achieved shearing the Solid bearing to approximately 160% shear strain. There was usually only one to three recycles per increment.

Stiffness Comparison

Values used in calculating the Table 2 stiffnesses were $A = \pi[(r_S + \Delta r_S)^2 - r_h^2]$, $G = 0.4061$ MPa and $K = 2030.5$ Mpa where Δr_S is the change in radius due to the cover rubber.

Comparisons of K_C values for the Solid bearing with and without cover rubber (Billings, 1992) reveals that use of $\pi(r_S + \Delta r_S)^2)$ improves the accuracy of the stiffness calculations as compared to omitting the cover rubber altogether. However, it overestimates the stiffening effect of the side cover layer. This correction term has been used throughout the calculations, as was the effect of bulk compliance given by equation (4). The same factors for side cover layer and bulk compliance were also used to determine the apparent values of F given in Fig. 2. This Figure was derived from comparison of the FEA stiffness for bearings with a central hole to that of the Solid bearing with the cover removed (Billings, 1992). The discrepancy between FEA results for F and equation (8) is substantial, especially at high values of r_S/r_h (i.e. small holes). This discrepancy is greater than can be attributed to the approach used to calculate the cover rubber's influence.

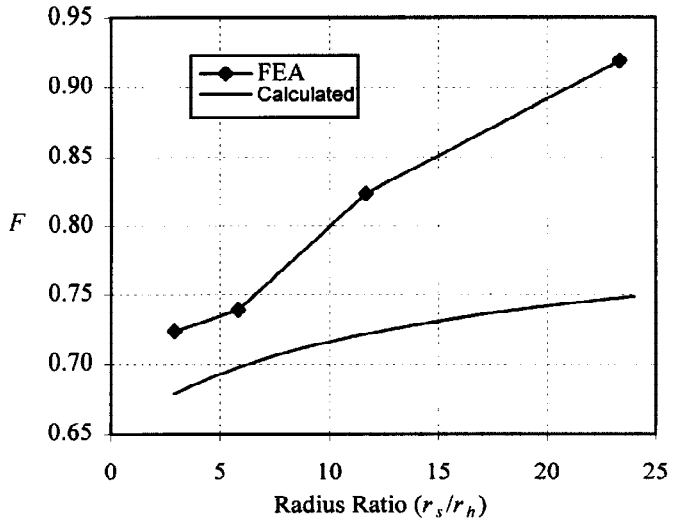

Fig. 2. Factor, F, for bearings with central holes.

Table 2 gives the FEA secant stiffnesses for shear deflection of the various bearings. The discrepancy between FEA and calculated values of K_S for the Solid bearing is surprisingly large in view of the good

Table 3. Stresses under Compression.

5.1 Mpa Compression	
	σ_{vm} (MPa) FEA
Solid	28.88
6 mm Hole	29.22
12 mm Hole	24.85
12 mm Filled Hole	44.88
24 mm Hole	23.84
48 mm Hole	22.30

Table 4. Stresses under Compression plus Shear

5.1 Mpa Compression plus 85% Shear Strain	
	σ_{vm} (MPa)
Solid	147.2
6 mm Hole	152.5
12 mm Hole	207.7
12 mm Filled Hole	148.1

agreement for K_C. In Table 2, the calculation of K_S for bearings with holes is based on that for the Solid bearing, but uses $A = \pi((r_S + \Delta r_S)^2 - r_h^2)$ rather than $\pi(r_S + \Delta r_S)^2$. This allows the cover rubber and central hole to be accounted for in the equations. This was necessary because there is no simple equation for the case of bearings with a central hole. This simple adjustment, assuming proportionality of K_S with the area of rubber, gives a guide as to the effect of the hole on the shear stiffness. It is apparent that for the 48 mm Hole bearing, the shear stiffness is significantly less than expected on the basis of the area of rubber.

Stress Comparison

A comparison of the maximum Von-Mises stress for the bearings esamined is given in Table 3 and Table 4.

From Table 3, the presence of a hole does not greatly affect the vulnerability of the plate to yield if the bearing is compressed, but filling the hole with rubber does increase the vulnerability. This effect is not observed under combined compression and shear (Table 4), from which it appears that there is little effect of a hole on yielding of the shim, provided the hole is filled with rubber.

CONCLUSIONS

Overall, the work reported in this paper has shown broad agreement between simple design equations and FEA. No design equations are currently available for determining the Von-Mises stress in the shims for bearings with central holes and for bearings under combined compression and shear. The FEA has provided this information which is presentable in color contour plots, giving graphic insight for a designer (Billings, 1992).

The agreement between the FEA and the closed form calculations of stiffness for bearings with a central hole was not good. Further investigation is called for to elucidate the cause of this discrepancy. A design curve derived from the FEA is provided in Fig. 2 as an improvement to the compressive stiffness reduction factor, F, found in the vertical stiffness equation, (8).

The understanding of the mechanics of elastomeric bearings has been advanced as a result of the work reported. The existing closed form design formulae appear adequate up to medium strain levels and are suitable for preliminary design applications.

ACKNOWLEDGMENTS

The authors wish to thank Alan Muhr and Hamid Ahmadi of the MRPRA for providing equations appropriate to the mechanics of elastomeric bearings and for supplying test data on the shear stress-strain properties of the rubber used in the bearings. The continued interest of Ian G. Buckle of the National Center for Earthquake Engineering Research is recorded with gratitude.

This research was supported in part by the University of California, Irvine, through an allocation of computer resources, and in part by the National Center for Earthquake Engineering Research, by way of financial support of the first author during his Ph.D. studies.

REFERENCES

Ahmadi, H. (1991). Personal communication, Malaysian Rubber Producers' Research Association.

Aiken, I. D., J. M. Kelly, P. W. Clark, K. Tamura, M. Kikuchi, and T. Itoh (1992). Experimental studies of the mechanical characteristics of three types of seismic isolation bearings. *Proc. Tenth World Conf., Earthquake Eng.*, pub. Balkema, Rotterdam.

Billings, L. J. (1992). *Finite Element Modeling of Elastomeric Seismic Isolation Bearings*, Ph.D. Thesis, University of California, Irvine.

Chalhoub, M. and J. M. Kelly (1986). Reduction of the stiffness of rubber bearings due to compressibility, *Report no. UCB/SESM-86/06*, University of California, Berkeley, CA.

Constantinou, M. C., A. Kartoum and J. M. Kelly (1992). Analysis of compression of hollow circular elastomeric bearings, *Eng. Struct.*, 14, 103-111.

Gent A. N. and E. A. Meinecke (1970). Compression, bending and shear of bonded rubber blocks. *Polymer Eng. and Science*, 10, 48-53.

Konter, A. (1993). MARC Analysis Research Corporation, personal communication.

Muhr, A. G. (1993). Malaysian Rubber Producers' Research Association, personal communication.

Rivlin, R. S. (1948). Large elastic deformations of isotropic materials IV, further developments of the general theory. *Phil. Trans. Roy. Soc.* 241A, 279,

Thomas, A. G. (1983). The Design of Laminated Bearings. *Proc. Int. Conf. On Natural Rubber for Earthquake Protection of Buildings*, ed. C. J. Derham, Publ. MRRDP (Kuala Lumpur).

Treloar, L. (1975). *The Physics of Rubber Elasticity*, Clarendon Press, Oxford, 3rd ed.

Yeoh, O. H. (1990). Characterization of elastic properties of carbon black filled rubber vulcanizates. *Rubb. Chem. Tech.* 63, 792-805.